Freeze-form Extrusion Fabrication of Functionally Graded Material Composites Using Zirconium Carbide and Tungsten

Ang Li, Aaron S. Thornton, Bradley Deuser, Jeremy L. Watts, Ming C. Leu,
Gregory E. Hilmas, Robert G. Landers
Missouri University of Science and Technology, Rolla, MO 65409
REVIEWED, Accepted August 20, 2012

Abstract

Ultra-high-temperature ceramics are being investigated for future use in aerospace applications due to their superior thermo-mechanical properties, as well as their oxidation resistance, at temperatures above 2000°C. However, their brittleness makes them susceptible to thermal shock failure. As graded composites, components fabricated as functionally-graded materials (FGMs) can combine the superior properties of ceramics with the toughness of an underlying refractory metal. This paper discusses the grading of two materials through the use of a Freeze-form Extrusion Fabrication (FEF) system to build FGM parts consisting of zirconium carbide (ZrC) and tungsten (W). Aqueous-based colloidal suspensions of ZrC and W were developed and utilized in the FEF process to fabricate test bars graded from 100%ZrC to 50%W-50%ZrC (volume percent). After FEF processing, the test bars were co-sintered at 2300°C and characterized to determine their resulting density and microstructure. Four-point bending tests were performed to assess the flexural strength of the test bars made using the FEF process, compared to that prepared using conventional powder processing and isostatic pressing techniques, for five distinct ZrC-W compositions. Scanning electron microscopy (SEM) was used to examine the inner structure of composite parts built using the FEF process.

1. Introduction

Fabrication of a functionally graded material (FGM) part refers to the process of manufacturing a part with multiple materials in a graded fashion in order to take advantage of complementary material properties while minimizing residual stresses that may result from the sintering process [1]. Ceramics are often used in high-temperature applications for their superior heat resistance; however, poor fracture toughness limits their use in high-stress scenarios and they are often difficult to manufacture for complex geometries using traditional processes. Several additive manufacturing technologies have been developed in recent years that can fabricate ceramic components with complex geometries, but few have the ability to build FGM parts.

Additive manufacturing (AM) technology has evolved since its inception in the mid 1980's, from polymer-based processes to metal-based and ceramic-based processes. Stereolithography [2], Fused Deposition Modeling [3], 3D Printing [4], and Selective Laser Sintering [5,6] are among the popular AM technologies practiced in industry today. The current metal and ceramic AM technologies are mostly limited to single material (monolithic) part fabrication. Robocasting [7], Extrusion Freeform Fabrication [8], Shape Deposition Manufacturing [9], and Laser Metal Deposition [10] are more apt in their potential to building multiple-material parts since they are deposition-based processes.

This study considers a novel additive manufacturing technology called Freeze-form Extrusion Fabrication (FEF), which is capable of producing three-dimensional parts by depositing aqueous-based ceramic and metal pastes in a layer-by-layer manner within a sub-zero temperature environment to minimize the amount of organic binder necessary, thus making post-processing easier and more environmentally friendly [11-15].

Some key components in aerospace applications demand extremely high performance, such as the leading edges of hypersonic vehicles, missile nose cones, and nozzle throat inserts for spacecraft propulsion systems. These components must be able to withstand extremely high temperatures (> 2000°C) and be integrated with underlying substructures, which are typically made of metals such as aluminum or titanium. To achieve these demanding characteristics, one approach is to build these components while grading from a ceramic to a metal. The grading should be done in a gradual fashion so as to minimize the thermal stresses generated due to different thermal expansion coefficients between the different materials, both during part fabrication and when the part is in service. Deposition-based additive manufacturing processes are advantageous for fabricating such components with functionally graded materials.

This paper considers the sintering of ZrC-W composite parts fabricated by the FEF process. As a refractory metal with a melting point of 3422°C and yield strength of approximately 800 MPa at room temperature[17], W shows great potential in aerospace applications, such as re-entry components, uncooled liquid rocket chambers, rocket nozzles, electrical propulsion components, etc. However, dramatic decreases occur in the mechanical strength of W with increases in temperature. For example, the mechanical strength of W decreases by ~60% when heated from room temperature to 1000°C [17]. To enhance the mechanical strength of W at elevated temperatures, ZrC can be introduced as a reinforcement material because of its high melting temperature (3532°C) and thermal expansion coefficient similar to that of W [18]. Several methods have been used for the fabrication of ZrC-W composites, the most typical one being hot pressing [18]. A high relative density can be achieved by the hot pressing method (> 98%); however, the dimensional limitation narrows the scope of applications for this method. An in-situ reaction sintering process was able to achieve a relative density of approximately 94.5% for the manufacture of ZrC-W composites without applying external pressure during sintering [19]. In this paper, we compare the relative densities, flexural strengths, and microstructures of test bars of different ZrC and W compositions fabricated by the FEF process and by a traditional powder processing route that includes isostatic pressing. The test bars were sintered at temperatures ranging from 2100 to 2300°C in attempts to achieve the highest possible relative densities.

2. Freeze Form Extrusion Fabrication Process Overview

An FEF machine equipped with three servo controlled extruders and a three-axis gantry motion system in a temperature-controlled enclosure has been developed, as shown in Figure 1. The FEF machine is equipped with a triple-extruder mechanism to build three-dimensional FGM parts with complex geometries. The different materials are combined by feeding them into an inline static mixing unit and output the mixed pastes through a single orifice. This static mixer forces the pastes to mix together before exiting the orifice, and provides a natural transition between paste composition changes. The different pastes are extruded simultaneously by controlling the velocity of each plunger. As an example, assuming that the three cylinders contain three different pastes and have the same cross-sectional area, a desired paste mixture

consisting of 20% paste A, 30% paste B, and 50% paste C can be achieved by controlling the three plunger velocities with the ratios of v_1:v_2:v_3 = 2:3:5, where v_1, v_2, and v_3 are the plunger velocities for pastes A, B, and C, respectively. The mixed colloidal paste is deposited onto a solid substrate layer by layer within a sub-zero temperature environment (-10°C in our present study). Following the FEF fabrication, the fabricatedpart is transferred to a freeze-dryer to sublime excess water from the green part and then undergoes binder burnout and sintering.

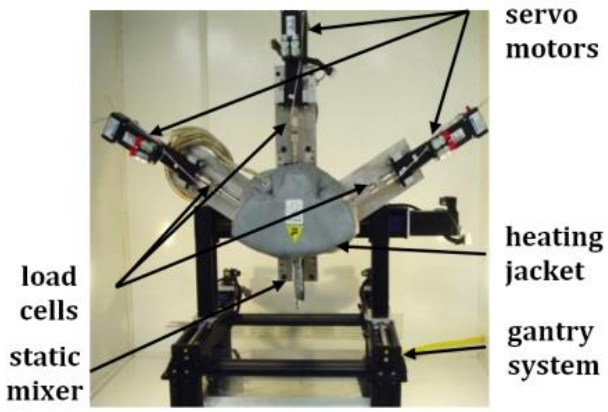

Figure 1. The triple-extruder Freeze-form Extrusion Fabrication (FEF) machine.

3. Materials Processing

3.1. Characterization of Sintering Behavior

In order to achieve acceptable mechanical properties, ZrC-W composites produced by the FEF process will require a high temperature sintering cycle to achieve the highest possible relative density. The co-sinterability of ZrC and W was investigated by fabricating several batches of test pellets with the composition of 50vol%ZrC+50vol% W and sintering at different temperatures and heating rates (as shown in Table 1).

Table 1. Heating conditions for co-sintering test.

Temperature	Holding time	Atmosphere	Heating rate	Relative density
2100°C	1 hour	Helium	10 °C/min	74.51%
2300°C	1 hour	Helium	10 °C/min	71.52%
2300°C	3 hours	Helium	10 °C/min	80.71%
2300°C	3 hours	Helium	10°C/min from room temperature to 2100°C, and then 2°C/min to 2300°C	78.45%

During the experiments, the powders of ZrC (＜2μm, Grade B, H.C. Starck, Karlsruhe, Germany) and W (0.6~1μm, Sigma Aldrich, St. Louis, MO) were first mixed and ball-milled using acetone and zirconia media for 2 hours. After ball milling, the slurry was dried by rotary evaporation (Buchi, Flawil, Germany) at a temperature of 70°C, low vacuum (~27 kPa), and a

rotation speed of 60 rpm. The dry powder was ground, filtered through a 180μm sieve, and pressed into pellets using a hydraulic press with a half-inch diameter die at 2000 psi. The pellets were then isostatically pressed at 30,000 psi before sintering. Sintering was performed in a graphite furnace (Thermal Technology, Santa Rosa, CA) under a helium atmosphere. The densities of the sintered pellets were determined using the Archimedes method, and each pellet was polished for scanning electron microscopy (SEM, S4700 and S570, Hitachi, Tokyo, Japan). Figure 2 shows the pressed and sintered pellets.

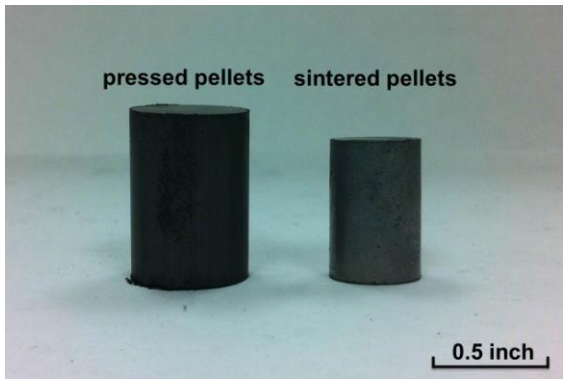

Figure 2, Pressed and sintered pellet.

The sintering of the pellets (co-sintering of ZrC and W) was performed under four different heating conditions, which are listed along with the resulting relative density data in Table 1. Maintaining a heating rate of 10°C/min while increasing the sintering temperature from 2100°C to 2300°C was found to increase the relative density from ~71% to ~81% (see Table 1). However, a relative density above 81% could not be achieved despite additional modifications to the sintering cycle. SEM analysis of a sample with the highest relatively density (~81%) showed many visible pores in the ZrC phase as seen in Figure 3, where ZrC is the darker phase and W is the lighter phase. This indicates that the rate of grain growth of ZrC was too fast under the current heating condition, causing entrapped pores and thus insufficient densification of ZrC.

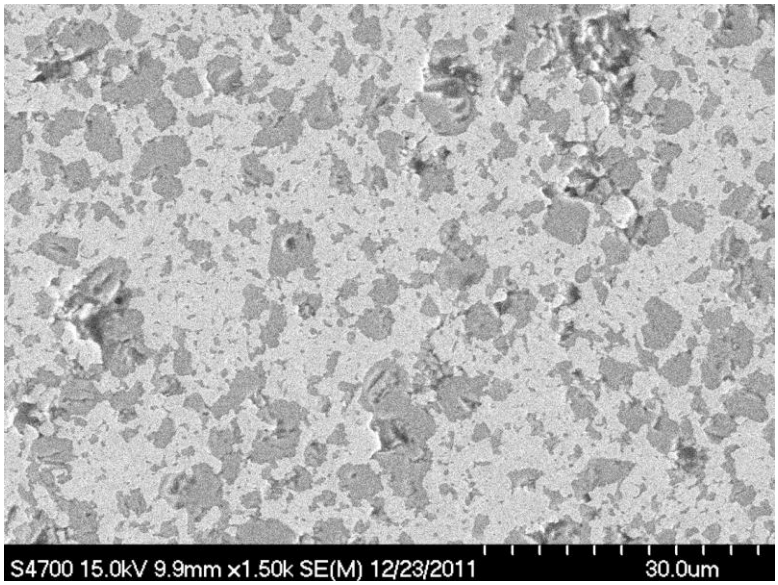

Figure 3. SEM images of 50%ZrC+50%W pellets with relative density of 80.71%.

Table 2. Comparison between as-received and attrition-milled ZrC powders.

ZrC powder	Average particle size (μm)	BET surface area (m^2/g)
As-received	0.47	1.06
Attrition-milled	0.35	6.13

To verify the effect of attrition milling on the sinterability of ZrC, another batch of pellets was made with the composition of 50vol%ZrC+50vol%W and 90vol%ZrC+10vol%W using the attrition milled ZrC powder. Also, one batch of 90vol%ZrC(as-received)+10vol%W pellets were also produced for comparison. The sintering test was conducted at a heating rate of 10°C/min from room temperature to 2100°C, and then 2°C/min to 2300°C in order to allow for more time at the lower sintering temperatures and limit ZrC grain growth.

The pellets made with the attrition-milled ZrC powder resulted in a significant increase in density compared with the pellets made with the as-received ZrC powder (Table 3). The 50vol%ZrC+50vol%W composition achieved a 98.9% relative density, while the 90vol%ZrC+10vol%W composition achieved a relative density of 99.4%. Figure 4 shows SEM images for 50vol%ZrC+50vol%W pellets made with the as-received and attrition-milled ZrC powders. Based on SEM analysis, it is clear that attrition milling not only contributed to a higher material density after sintering, but also decreased the ZrC and W grain sizes as well as the number and size of pores inside the sintered parts. Thus, the sintered pellets made with attrition-milled ZrC powder resulted in a higher density and finer microstructure.

Table 3. Comparison between sintered pellets made with as-received and attrition-milled ZrC powders.

Composition	Relative density (with as-received ZrC)	Relative density (with attrition-milled ZrC)
50vol%ZrC+50vol%W	78.45%	98.9%
90vol%ZrC+10vol%W	71.32%	99.4%

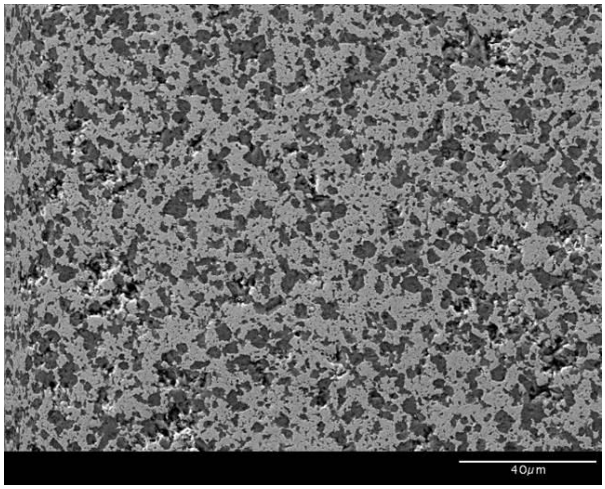

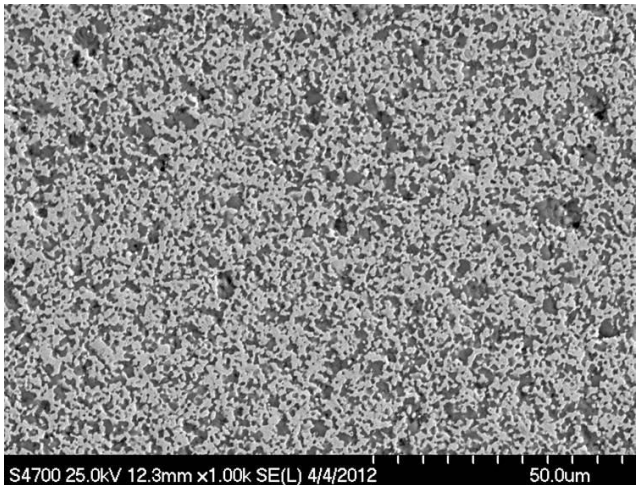

(a) (b)

Figure 4. (a). Microstructure of 50vol%ZrC+50vol%W pellets made from as-received ZrC powder. (b). Microstructure of 50vol%ZrC+50vol%W pellets made from attrition-milled ZrC powder.

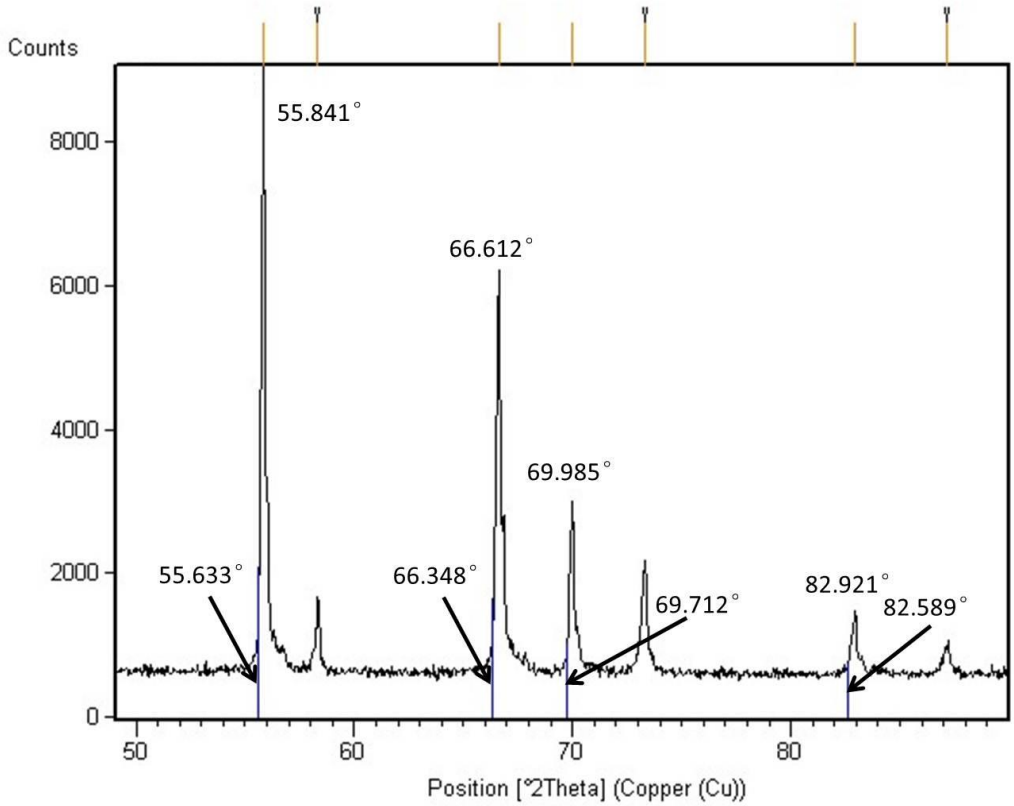

Figure 5. XRD analysis on ZrC/W pellets.

The sintered ZrC/W pellets, made using the attrition-milled ZrC powder, were ground back to powder for X-ray diffraction (XRD) analysis (XDS 2000, Scintag Inc., Cupertino, CA). The XRD results are presented in Figure 5. The detected highest-intensity ZrC peaks (55.841^o, 66.612^o, 69.985^o and 82.921^o) in the XRD patterns were all shifted to higher two-theta angles compared to the reference peaks (55.633^o, 66.348^o, 69.712^o and 82.589^o). An increase in the two-theta angle indicates a decrease in lattice parameter in the ZrC unit cell, implying that there was formation of (Zr,W)C solid solution. This is not an unexpected result and has been previously observed in the technical literature for ZrC-W systems [19].

3.2. Development of ZrC and W Pastes

To ensure a stable viscosity during FEF deposition and good mechanical strength of parts made by the FEF process, many tests were conducted on the development of ZrC and W pastes. Most important to these tests were the investigation of appropriate dispersants, which control the rheological behavior of the pastes. W powder was found to be particularly difficult to disperse in aqueous solutions due to its high density (19.25 g/cm^3). After an initial set of experiments

involving several dispersants, it was determined that Sodium Dodecyl Sulfate (SDS, Sigma Chemical Co, St. Louis, MO) could disperse the W powder in distilled water at a solids loading of ~45 vol%. Further, SDS also performed well in dispersing ZrC powder to ~50 vol% solids loading in distilled water. Thus SDS was selected as the dispersant to produce pure ZrC and 50vol%ZrC+50vol%W pastes at solids loadings of 50 vol%. After each powder composition was dispersed in water, hydroxypropyl methylcellulose (Methocel, The Dow Chemical Company, Midland, Michigan) was added to the slurries as the binder to control the paste viscosity. The amount of dispersant and binder were controlled to ensure paste viscosities that suited the FEF machine. During the FEF fabrication, the viscosity of pastes was adjusted based on the extrusion force of the plunger by keeping the extrusion force in the range between 600N and 900N. The pastes were then extruded by FEF machine to fabricate test bars for flexural strength testing.

4. FEF Test Bar Fabrication

Test bars of five different compositions were fabricated using the FEF process, among which three compositions, 12.5vol%W+87.5vol%ZrC, 75vol%W+25vol%ZrC and 37.5vol%W+62.5vol%ZrC, were deposited by mixing of the two initial pastes (100vol%ZrC and 50vol%ZrC+50vol.%W) in various ratios. Five additional test bars were made using an isostatic press after mixing W and attrition-milled ZrC powders into the desired compositions in order to compare their mechanical properties. The process of fabricating test bars was the same as that for pellets. After sintering, these test bars were cut and ground into 3×4×45 mm^3 pieces according to ASTM C 1161-02c for type B bars.

Table 4. Measured properties of FEF fabricated and iso-pressed test bars.

	FEF Fabricated		Isostatic Pressed	
Composition (vol.%)	Relative Density	Flexural Strength (MPa)	Relative Sintered Density	Flexural Strength(MPa)
100%ZrC	62.05%	73	98.49%	224
12.5%W+87.5%ZrC	47.89%	25	94.41%	265
25%W+75%ZrC	56.19%	25	97.34%	398
37.5%W+62.5%ZrC	47.28%	28	95.40%	414
50%W+50%ZrC	70.08%	31	99.81%	404

The data in Table 4 indicate that the flexural strength of the isostatic pressed bars increased with a higher concentration of W, from 224 MPa for 100% ZrC to 404 MPa for the 50%ZrC+50%W composition. This result implies that the W played an important role in increasing the flexural strength of the composites. However, this trend was not observed for the FEF fabricated bars. The relative density and flexural strength of FEF fabricated bars were, in general, much lower than those of the isostatic pressed bars. In order to have a better understanding of the differences, SEM images were taken to compare the microstructures of the test bars. From the SEM analysis (Figure 6), many large pores (10's to 100's of μm) were present in the bars produced by the FEF process, and the pores became even more severe with increasing ZrC content. However, all of the isostatic pressed bars show highly densified microstructures, with the relative densities of all test bars above 94% and the 50%ZrC+50%W composition achieving 99.8% in relative density.

There are two reasons that can be used to explain for the severe porosity in the FEF fabricated bars. The first reason is that the static mixer did not do an adequate job of mixing the pastes, leading to significant variations in the materials compositions and differential sintering at different locations within the test bars. Figure 7 shows the cross sections of FEF fabricated test bars with 62.5%ZrC+37.5%W and 87.5%ZrC+12.5%W. Clearly visible in the images are marked differences in the intended compositions at different locations. The ZrC-rich areas (darker phase) are distinct from W-rich areas (lighter phase), indicating the insufficient paste mixing during the extrusion. The second and more critical reason for the porosity is that during the FEF process large ice crystals were formed as the water was freezing. This has been shown in previous studies of aqueous based freeze casting of ceramics wherein large ice crystals are formed, resulting in large voids (100's of μm) after sintering [20]. Once formed during the freezing process, these large defects remained inside the test bars, affecting the final mechanical properties. An example is given in Figure 8, which shows the formation of what appears to be the remnants of ice crystals in the 100%ZrC sample after freeze drying. As has been discussed by Sofie and Dogan [20], these voids may be controlled, or even eliminated, in the future through the use of glycerol additions to the aqueous based slurries. .

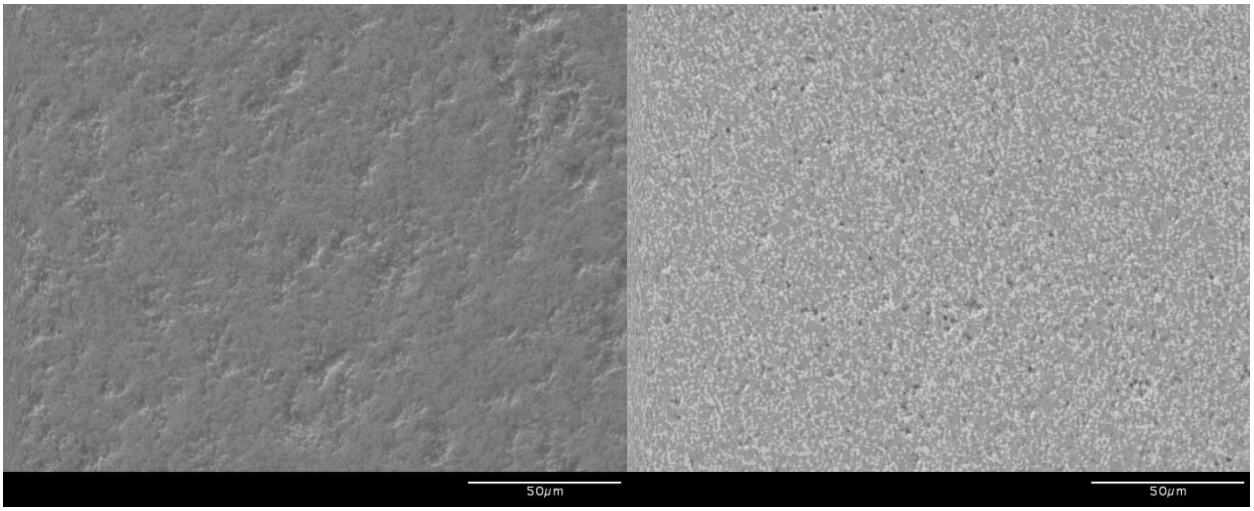

(a) (b)

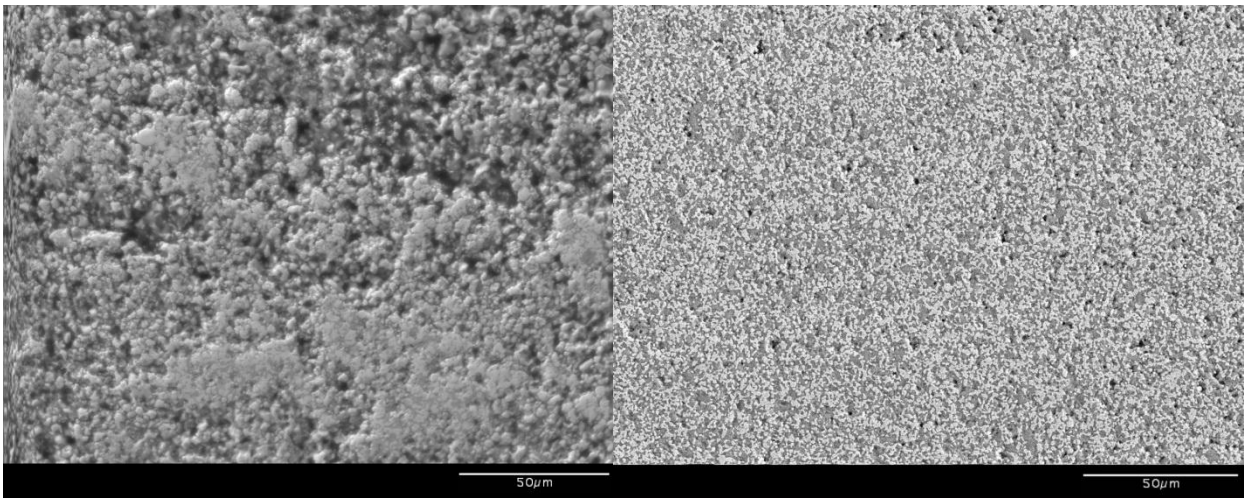

(c) (d)

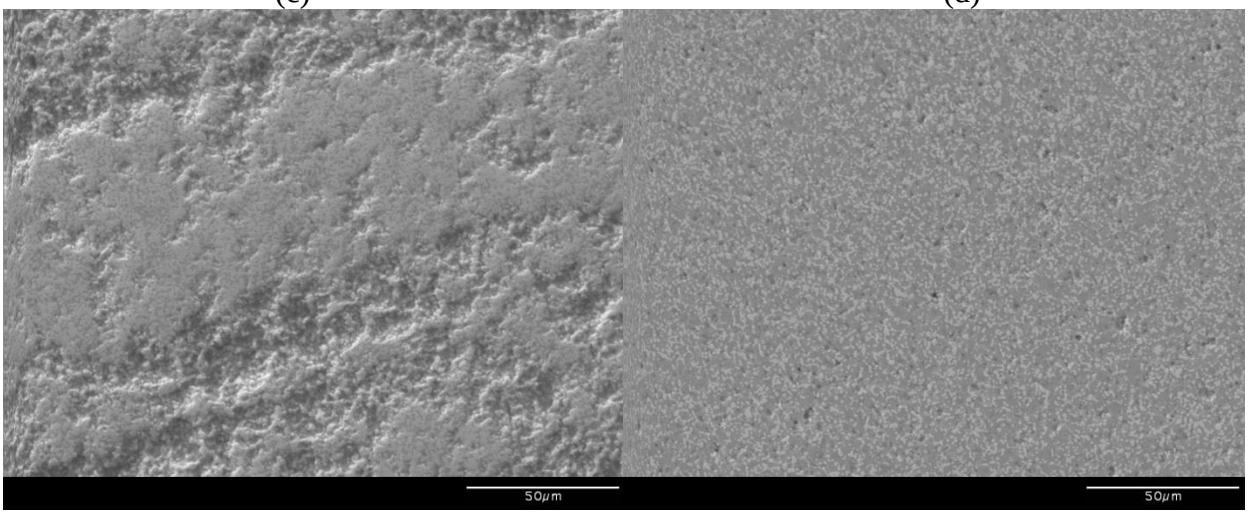

(e) (f)

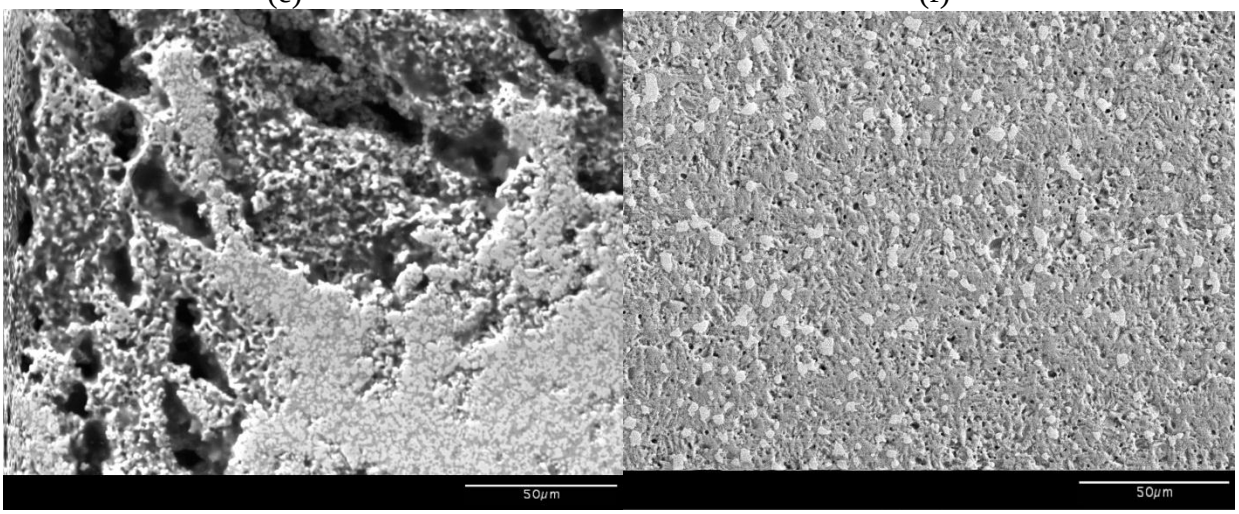

(g) (h)

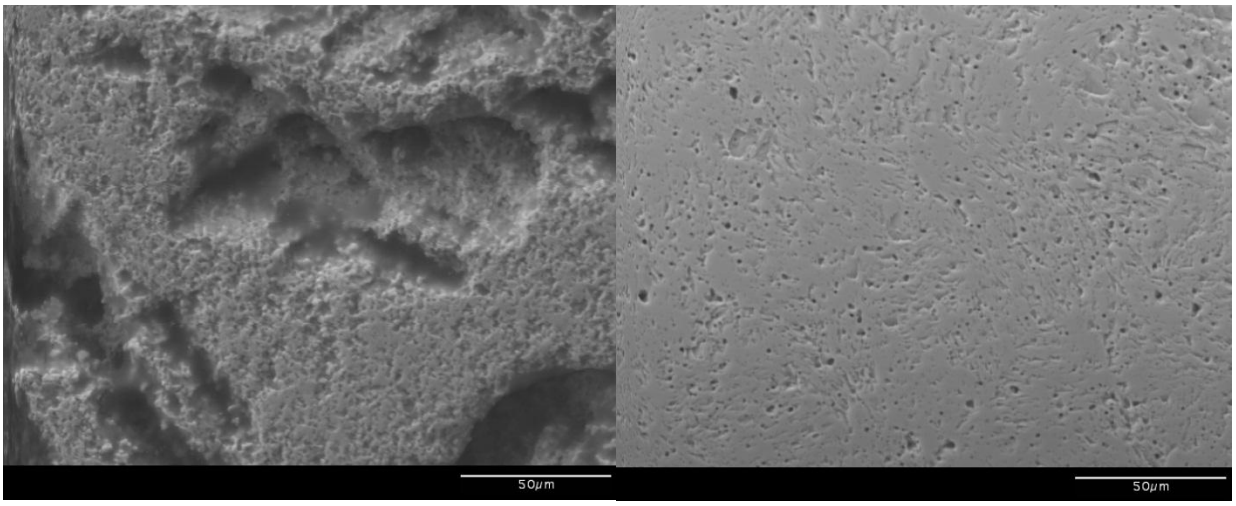

(i) (j)

Figure 6. SEM images of the micro-structure of (a). 50%ZrC+50%W, FEF fabricated; (b). 50%ZrC+50%W, isostatic pressed; c). 62.5%ZrC+37.5%W, FEF fabricated; (d). 62.5%ZrC+37.5%W, isostatic pressed; (e). 75%ZrC+25%W, FEF fabricated; (f). 75%ZrC+25%W, isostatic pressed; (g). 87.5%ZrC+12.5%W, FEF fabricated; (h). 87.5%ZrC+12.5%W, isostatic pressed; (i). 100%ZrC, FEF fabricated; (j). 100%ZrC, isostatic pressed.

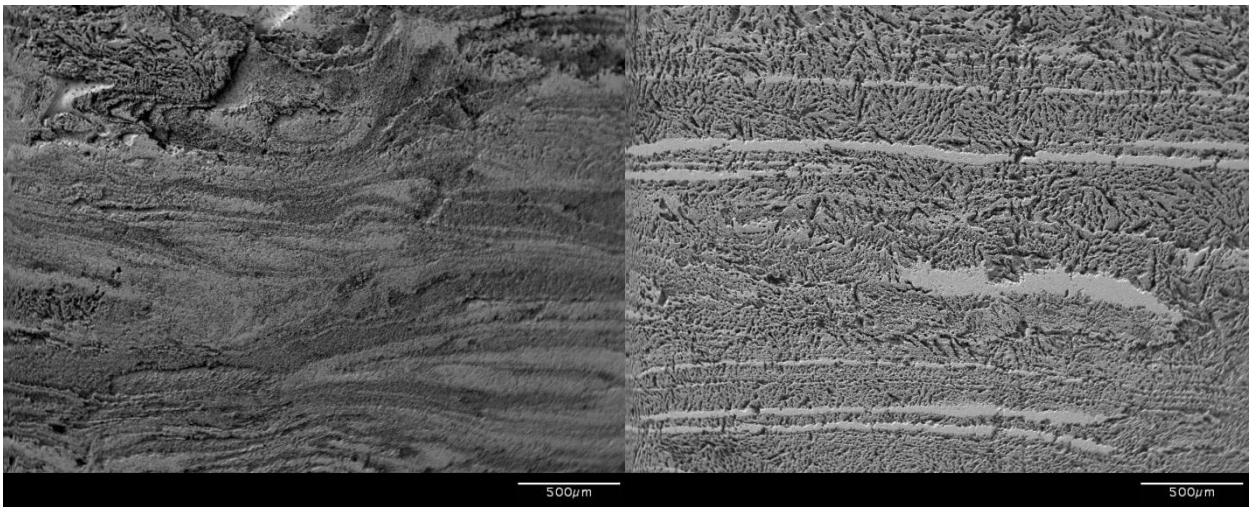

(a) (b)

Figure 7. SEM images of FEF test bars: (a). Cross section of 62.5%ZrC+37.5%W. (b). Cross section of 87.5%ZrC+12.5%W.

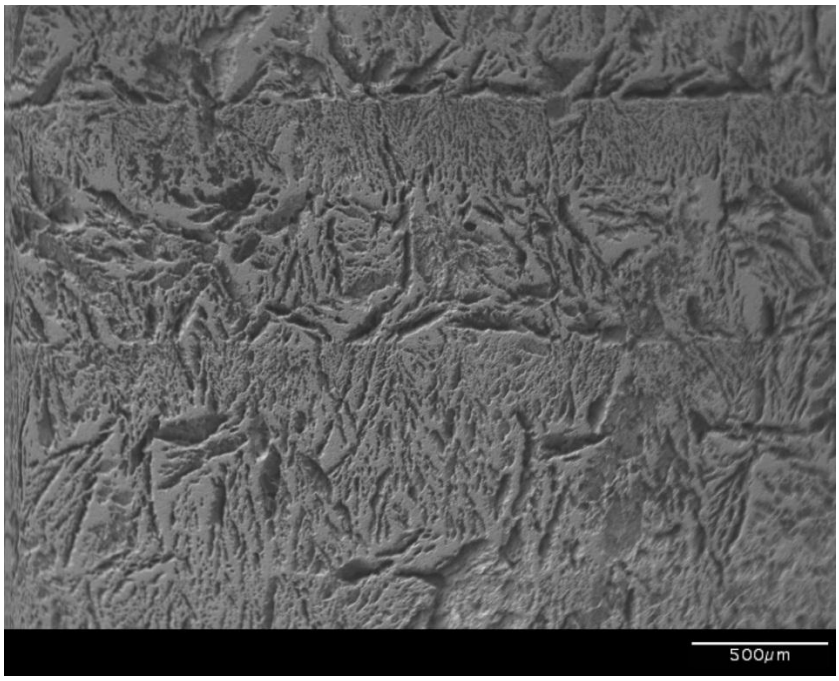

Figure 8. SEM image showing the formation of ice crystals in the FEF-fabricated 100%ZrC test bar.

5. Summary and Conclusions

ZrC/W test bars with compositions ranging from 100% ZrC to 50%ZrC+50%W by volume were prepared by isostatic pressing and freeze-form extrusion fabrication (FEF). Using attrition milled ZrC powder, relative densities ranging from 94.4% to 99.8% could be achieved for isopressed and co-sintered ZrC and W compositions by sintering at 2300°C at the heating rate of 10°C/min from room temperature to 2100°C, and then 2°C/min to 2300°C. However, FEF fabricated bars only achieved 47-70% relative density for similar compositions. Flexural strength data from four-point bending tests followed a similar trend, with strengths in the range of 200-400 MPa for the dense isopressed bars and strengths of only 25-70 MPa for the bars produced by FEF processing. The large differences in both density and flexure strength between the isostatic pressed and FEF fabricated test bars were found to be due to large voids inside the FEF fabricated bars from the formation of ice crystals during the freezing process. Elimination of these large voids, combined with an improved mixing method, are needed in order to enhance the performance of graded ZrC/W composites fabricated by the FEF process.

6. Acknowledgements

This project is funded by NSF grant #CMMI-0856419 with matching support from the Boeing company through the Center for Aerospace Manufacturing Technologies at the Missouri University of Science and Technology, and by the Air Force Research Laboratory contract #10-S568-0094-01-C1 through the Universal Technology Corporation.

7. References

[1] Kruth, J.P., Leu, M.C., Nakagawa, T., 1998, Progress in Additive Manufacturing and Rapid Prototyping, CIRP Annals - Manufacturing Technology, 47/2:525-540.
[2] Levy, G.N., Schindel, R., Kruth, J.P., 2003, Rapid Manufacturing and Rapid Tooling with Layer Manufacturing (LM) Technologies, State of the Art and Future Perspectives, CIRP Annals - Manufacturing Technology, 52/2:589-609.
[3] Bandyopadhyay, A., Panda, P., Agarwala, M., Danforth, S., Safari, A., 2000, Processing of Piezocomposites by Fused Deposition Technique, Journal of the American Ceramic Society, 80/6:1366-1372.
[4] Crump, S., 1992, Apparatus and Method for Ceramic Three-Dimensional Objects, U.S. Patent No. 5121329.
[5] Hilmas, G.E., Lombardi, J., Hoffman, R., Advances in the Fabrication of Functional Graded Materials Using Extrusion Freeform Fabrication, Proceedings of Solid Freeform Fabrication Symposium, University of Texas at Austin, August 1996.
[6] Cima, M., Oliveira, M., Wang, H., Sachs, E., Holman, R., 2001, Slurry-Based 3DP and Fine Ceramic Components, Proceedings of Solid Freeform Fabrication Symposium.
[7] Kruth, J., Mercelis, P., Froyen, L., Rombouts, M., 2004, Binding Mechanisms in Selective Laser Sintering and Selective Laser Melting, Proceedings of Solid Freeform Fabrication Symposium.
[8] Leu, M.C., Adamek, E., Huang, T., Hilmas, G.E., Dogan, F., 2008, Freeform Fabrication of Zirconium Diboride Parts Using Selective Laser Sintering, Proceedings of Solid Freeform Fabrication Symposium.
[9] Stampfl, J., Cooper, A., Leitgeb, R., Cheng, Y., Prinz, F., 2001, Shape Deposition Manufacturing of Microscopic Ceramic and Metallic Parts Using Silicon Molds, U.S. Patent, No. 6242163.
[10] Cesarano III, J., Segalmen, R., Calvert, P., 1998, Robocasting Provides Moldless Fabrication from Slurry Deposition, Ceramics Industry, 148:94-102.
[11] He, G., Hirschfeld, D., Cesarano III, J., Stuecker, J., 2000, Processing of Silicon Nitride-Tungsten Prototypes, Ceramic Transactions, 114:325-332.
[12] Huang, T., Mason, M.S., Hilmas, G.E., Leu, M.C., 2006, Freeze-form Extrusion Fabrication of Ceramic Parts, International Journal of Virtual and Physical Prototyping, 1/2:93-100.
[13] Mason, M.S., Huang, T., Landers, R.G. Leu, M.C., Hilmas, G.E. , 2009, Aqueous-Based Extrusion of High Solids Loading Ceramic Pastes: Process Modeling and Control, Journal of Materials Processing Technology, 209/6:2946-2957.
[14] Huang, T., Mason, M.S., Hilmas, G.E., Leu, M.C., 2009, Aqueous Based Freeze-form Extrusion Fabrication of Alumina Components, Rapid Prototyping Journal, 15/2:88-95.
[15] Zhao, X., Landers, R.G., Leu, M.C., 2010, Adaptive Extrusion Force Control of Freeze-Form Extrusion Fabrication Processes, ASME Journal of Manufacturing Science and Engineering, 132/6:064504.
[16] Doiphode, N.D., Huang, T., Leu, M.C., Rahaman, M.N., Day, D.E., 2011, Freeze Extrusion Fabrication of 13-93 Bioactive Glass Scaffolds for Bone Repair, Journal of Material Science: Materials in Medicine, 22/3:515-523.
[17] Yih, S.W. and Wang, C.T., 1979 Tungsten-Sources, Metallurgy, Properties and Application. Plenum Press, New York.

[18] Song, G.-M., Wang, Y.-J., Zhou, Y., 2002, The Mechanical and Thermophysical Properties of ZrC/W Composites at Elevated Temperature, Materials Science and Engineering: A, 334:223–232.
[19] Zhang, S. C., Hilmas, G. E., Fahrenholtz, W. G., 2007, Zirconium Carbide–Tungsten Cermets Prepared by In Situ Reaction Sintering, Journal of the American Ceramic Society, 90/6:1930–1933.
[20] Sophie, S. W., Dogan, F., 2001, Freeze Casting of Aqueous Alumina Slurries with Glycerol, Journal of the American Ceramic Society, 84/7:1459–1464.